Venous Compression at High-Spatial-Resolution Three-dimensional MR Angiography of Peripheral Arteries[1]

Florian M. Vogt, MD
Waleed Ajaj, MD
Peter Hunold, MD
Christoph U. Herborn, MD
Harald H. Quick, PhD
Jörg F. Debatin, MD, MBA
Stefan G. Ruehm, MD

Index terms:
Arteries, stenosis or obstruction, 92.721
Extremities, angiography, 92.122, 92.12942
Extremities, MR, 92.12942
Magnetic resonance (MR), vascular studies, 92.12942

Published online before print
10.1148/radiol.2332031367
Radiology 2004; 233:913–920

Abbreviations:
CNR = contrast-to-noise ratio
DSA = digital subtraction angiography
GRAPPA = generalized autocalibrating partially parallel acquisition
SI = signal intensity
SNR = signal-to-noise ratio
3D = three-dimensional

[1] From the Department of Diagnostic and Interventional Radiology, University Hospital Essen, Hufelandstrasse 55, 45122 Essen, Germany (F.M.V., W.A., P.H., C.U.H., H.H.Q., J.F.D.); and Department of Radiology, David Geffen School of Medicine at UCLA, Los Angeles, Calif (S.G.R.). Received August 27, 2003; revision requested November 6; revision received January 21, 2004; accepted March 2. **Address correspondence to** F.M.V. (e-mail: *florian.vogt@uni-essen.de*).

Authors stated no financial relationship to disclose.

Author contributions:
Guarantors of integrity of entire study, F.M.V., S.G.R., J.F.D.; study concepts, F.M.V., S.G.R., J.F.D., P.H., W.A., H.H.Q.; study design, F.M.V., W.A., C.U.H., P.H., S.G.R., J.F.D.; literature research, F.M.V., S.G.R., H.H.Q.; clinical studies, F.M.V., W.A., S.G.R.; data acquisition, F.M.V., P.H., C.U.H., H.H.Q.; data analysis/interpretation, F.M.V., S.G.R., C.U.H., P.H., H.H.Q.; statistical analysis, F.M.V., S.G.R.; manuscript preparation, F.M.V., P.H., C.U.H., S.G.R., J.F.D., H.H.Q.; manuscript definition of intellectual content, revision/review, and final version approval, all authors; manuscript editing, F.M.V., S.G.R.

The aim of this study was to assess a venous compression technique that is performed with contrast material–enhanced peripheral magnetic resonance (MR) angiography to reduce venous enhancement. Healthy volunteers, as well as patients with correlating digital subtraction angiographic (DSA) findings, were examined. Venous compression was accomplished by placing a cuff at the midfemoral level unilaterally. Arterial signal-to-noise and contrast-to-noise ratios indicated no significant differences between compressed and noncompressed legs. Venous overlay was substantially reduced in the compressed legs. MR angiography with venous compression yielded diagnostic image quality and results that had excellent correlation with DSA findings. High-spatial-resolution peripheral MR angiography of improved diagnostic quality appears feasible, even with long data acquisition times.

Three-dimensional (3D) contrast material–enhanced magnetic resonance (MR) angiography has emerged as a robust, safe, and reproducible alternative to digital subtraction angiography (DSA) for the evaluation of peripheral vascular disease (1–5). Single-injection bolus-chase techniques with integrated table motion algorithms enable assessment of the pelvic and runoff arteries during a single examination (6–10). By enabling augmentation of signal-to-noise ratios (SNRs) and contrast-to-noise ratios (CNRs) in the lower extremity vessels, dedicated peripheral vascular coils have provided a means of delineating small trifurcation arteries (11,12). Despite these improvements, adequate visualization of the small distal trifurcation and pedal arteries remains difficult.

Thus, in most institutions, conventional DSA remains the modality of choice for the assessment of small distal arteries of the foot when surgical revascularization strategies are being considered (13). The implementation of MR angiographic techniques for this purpose has been complicated by the need for rapid data collection to avoid venous overlap. Thus, although the higher SNR that is inherent to small vessels when dedicated peripheral coils are used facilitates improved spatial resolution (11), the time constraints governing data acquisition during the arterial phase do not. In principle, two strategies can be used to address this dilemma: shortening the data acquisition time and lengthening the arterial phase time window. Although data collection times can be shortened by using parallel imaging techniques in the setting of a multistation protocol (14,15), lengthening of the arterial phase time window could be accomplished by implementing midfemoral venous compression (16).

Thus, the purpose of our study was to assess a venous compression technique that is performed with contrast-enhanced peripheral MR angiography to reduce venous enhancement.

Materials and Methods

Study Subjects

High-spatial-resolution peripheral MR angiography was performed in five healthy volunteers with no history of pe-

TABLE 1
Parameter Values Used to Examine Four Stations at MR Angiography

Parameter	Pelvis	Thighs	Lower Parts of Legs	Distal Legs, Feet
Repetition time (msec)	2.36	2.96	2.96	3.77
Echo time (msec)	0.96	0.97	1.25	1.37
Flip angle	20°	20°	20°	20°
Field of view (mm × mm)	370 × 400	370 × 400	375 × 400	350 × 400
Acquired section thickness (mm)	3.33	1.56	1.51	1.51
Interpolated section thickness (mm)	2	1	1	1
Section spatial resolution (%)	60	64	66	66
No. of sections	48	88	64	120
Partial Fourier transform phase	6/8	6/8	7/8	7/8
Acquired matrix	210 × 384	210 × 384	480 × 512	358 × 512
Interpolated matrix	460 × 768	422 × 768	952 × 1024	757 × 1024
Acquired voxel size (mm^3)	1.7 × 1.0 × 3.3	1.7 × 1.0 × 1.56	0.8 × 0.8 × 1.51	0.9 × 0.8 × 1.51
Interpolated voxel size (mm^3)	0.8 × 0.5 × 2	0.8 × 0.5 × 1	0.4 × 0.4 × 1	0.45 × 0.4 × 1
Bandwidth (Hz/pixel)	770	770	750	390
Acquisition time (sec)	13	15	24	44
Time to center k-space (sec)	3.6	4.9	7.7	17.1
Acceleration factor	0	2	2	2

ripheral vascular disease (according to physical examination results, medical records, and nonsmoking status) and in five patients consecutively referred for conventional DSA because they were suspected of having peripheral vascular disease. The five healthy volunteers were two men and three women with an average age of 31 years (age range, 26–37 years). The five patients were three men and two women with an average age of 45 years (age range, 22–72 years).

In all subjects, both lower extremities were imaged at the same time. To permit direct comparisons, midfemoral venous compression was applied to one leg, which was chosen randomly. This study was approved by the local institutional review board of University Hospital Essen, and informed consent was obtained from all subjects.

The five patients presented with different stages of peripheral vascular disease according to the Rutherford classification system (17). The disease stage in each limb ($n = 10$) was specified independently: Four limbs had grade I, category 1; three limbs had grade I, category 3; one limb had grade II, category 4; and two limbs had grade III, category 5 peripheral vascular disease. All patients underwent conventional DSA of the aortoiliac and lower extremity arteries 24–48 hours before undergoing MR imaging.

Conventional Angiography

Only the five patients underwent conventional nonselective DSA, which was performed by using an angiographic unit (Ultimax; Toshiba Medical Systems, Neuss, Germany) with a programmable moving table (matrix, 1024 × 1024). Nonionic iodinated contrast material, gadobenate dimeglumine (MultiHance; Bracco Diagnostics, Milan, Italy), was injected through a power injector (Spectris; Medrad, Pittsburgh, Pa) at a rate of 13–15 mL/sec and at a dose of 110–190 mL. All examinations were performed by using a 4- or 5-F pigtail catheter, which was placed in the distal aorta above the bifurcation. Anteroposterior projections were acquired at all levels. Oblique images of the pelvic and pedal regions also were obtained. The angiograms were assessed in consensus by two radiologists—S.G.R. and P.H.—who, respectively, had 5 and 10 years of experience and were blinded to the results of MR angiography.

MR Angiography

MR imaging was performed by using a 1.5-T system (Magnetom Sonata; Siemens, Medical Solutions, Erlangen, Germany) equipped with eight receiver channels and high-performance gradients characterized by an amplitude of 40 mT/m and a slew rate of 200 mT/m/msec. All subjects were placed in the unit feet first and were examined while in the prone position. The dedicated peripheral vascular coil (CP Peripheral Angio Array Coil; Siemens, Medical Solutions) that was used consisted of eight separate circularly polarized flexible elements: four on the right side and four on the left side. The total length of the coil in the z-axis direction was 950 mm, and the length of the cage was 900 mm. Thus, the coil covered both lower extremities from the inguinal ligament to the foot. To cover the lower part of the abdomen and the pelvis, we combined this coil with two phased-array surface coils and a spine-array coil. The use of commercially available floating-table MR angiography software (Siemens, Medical Solutions) ensured rapid motion from one imaging position to the next.

Based on multiplanar scout MR image findings, the acquisition of four overlapping 3D data sets was planned. The slabs for the pelvis, thighs, and lower parts of the legs were strictly coronal, whereas the slabs for the feet were angulated to cover the dorsal arteries of the feet and the plantar arch arteries. Data were collected by using a fast 3D T1-weighted gradient-echo sequence with linear k-space sampling and partial Fourier acquisition. MR imaging parameters were adapted for each station and are summarized in Table 1. Repetition times ranged from 2.36 to 3.77 msec, and echo times ranged from 0.96 to 1.37 msec.

Without use of parallel imaging, a voxel size of 1.7 × 1.0 × 3.3 mm^3 (interpolated to 0.8 × 0.5 × 2.0 mm^3) was achieved in the first station (ie, the pelvis) in an acquisition time of 13 seconds. For the three subsequent stations (ie, thighs, lower parts of the legs, and feet), the generalized autocalibrating partially parallel acquisition (GRAPPA) algorithm with an acceleration factor of 2 was implemented (18). With this technique, the spatial information contained in the individual elements of a phased-array coil was used before the Fourier transformation to partially replace the phase-encoding steps that normally would be performed by using gradients. Voxel sizes were reduced to 1.70 × 1.00 × 1.56 mm^3 (interpolated to 0.8 × 0.5 × 1.0 mm^3) for the thighs, to 0.80 × 0.80 × 1.51 mm^3 (interpolated to 0.4 × 0.4 × 1.0 mm^3) for

the trifurcation vessels, and to 0.90 × 0.80 × 1.51 mm^3 (interpolated to 0.45 × 0.40 × 1.00 mm^3) for the feet. Despite the use of a parallel imaging factor of 2, data acquisition times increased to 15, 24, and 44 seconds, respectively, for the thighs, lower parts of the legs, and feet.

Paramagnetic contrast material, 0.5 mol/L of gadobenate dimeglumine, was injected automatically (Spectris) through a 19-gauge catheter that had been placed in the antecubital vein. A weight-adjusted dose of 0.2 mmol per kilogram of body weight (range, 22–37 mL) was injected by using a biphasic protocol: The first third of the volume was injected at a rate of 1.3 mL/sec, whereas the remaining amount was administered at a rate of 0.5 mL/sec. A 20-mL saline flush administered at a rate of 0.5 mL/sec followed.

A test bolus technique was used to determine the contrast material arrival time. This technique enables real-time visualization of the contrast agent bolus arriving in the abdominal aorta. The operator manually started the acquisition of the 3D data sets when the contrast agent was detected in the upper part of the abdominal aorta. To enable image subtraction, each 3D data set was acquired twice: before contrast agent administration and during the arterial contrast phase. A rerun function permitted the acquisition of the second data set without the need for repeated adjustments or sequence loading. The first data set was subtracted from the contrast-enhanced data at each level by using Syngo, VA 2002 C software (Siemens, Medical Solutions). Rotated maximum intensity projections were rendered over a 180° sector with 45 reconstructions.

For venous compression performed in one randomly assigned leg, a 30-cm-wide thigh cuff (Speidel and Keller, Jungingen, Germany) was placed at the midfemoral level of one leg before the MR angiographic examination. The cuff was inflated after the precontrast angiogram was obtained and was manually adjusted to a pressure of 50 mm Hg by using a nonferromagnetic pressure gauge (Speidel and Keller). The cuff remained inflated until the end of the examination. A pressure of 50 mm Hg was chosen to induce compression on the basis of empiric considerations.

Image Evaluation

For qualitative analysis, the arterial tree was divided into the following 44 segments: segments 1 and 2, the bilateral common iliac arteries; segments 3 and 4, the bilateral external iliac arteries; segments 5 and 6, the bilateral common femoral arteries; segments 7 and 8, the proximal halves of the bilateral superficial femoral arteries; segments 9 and 10, the distal halves of the bilateral superficial femoral arteries; segments 11 and 12, the bilateral popliteal arteries; segments 13 and 14, the bilateral tibioperoneal trunks; segments 15 and 16, the proximal halves of the bilateral anterotibial arteries; segments 17 and 18, the distal halves of the bilateral anterotibial arteries; segments 19 and 20, the proximal halves of the bilateral peroneal arteries; segments 21 and 22, the distal halves of the bilateral peroneal arteries; segments 23 and 24, the proximal halves of the bilateral posterotibial arteries; segments 25 and 26, the distal halves of the bilateral posterotibial arteries; segments 27 and 28, the bilateral dorsal arteries of the feet; segments 29 and 30, the bilateral medial plantar arteries; segments 31 and 32, the bilateral lateral plantar arteries; segments 33 and 34, the bilateral palmar arterial arches; and segments 35–44, the bilateral plantar metatarsal arteries.

Two radiologists (F.M.V., C.U.H.), each with 4 years experience performing MR angiography, assessed in consensus each arterial segment depicted on the nonsubtracted source images obtained in the 10 subjects by using the following three-point grading scale: A grade of 3 indicated diagnostic arterial depiction without venous contamination; a grade of 2, diagnostic arterial depiction with mild venous overlap; and a grade of 1, nondiagnostic arterial depiction due to severe venous overlap.

Furthermore, MR angiogram sets (S.G.R. and P.H. in consensus) obtained in all 10 subjects and DSA image sets (F.M.V. and C.U.H. in consensus) obtained in the five patients were analyzed for the presence of vascular disease in a blinded order. The degree of stenosis in each vascular segment was characterized by using a four-point grading scale: A grade of 0 indicated a normal segment (ie, no stenosis); a grade of 1, 50% or less luminal narrowing; a grade of 2, more than 50% luminal narrowing; and a grade of 3, occlusion. When two or more areas of narrowing were present in one segment, the most severe lesion was used for subsequent grading and analysis. DSA results served as the reference standard.

Quantitative Evaluation

SNR and CNR values were calculated on the basis of findings on the nonsubtracted source images of all 44 arterial segments in each subject. Because it was not possible to delineate the entire venous system on all acquired image data sets—especially owing to decreased vessel diameter in the lower parts of the leg and a lack of enhancement in the compressed leg—SNR and CNR analyses were performed only in selected venous segments of both legs to evaluate the benefit of absent venous flow induced by compression.

Signal intensity (SI) measurements were performed by using 4–6-mm regions of interest that were placed by the same author (F.M.V.) in the center of all 44 arterial vessel segments and of selected venous segments. This vessel region of interest was the region with the highest but also homogeneous SI (SI_{ves}). SI was also measured in a reference area in the adjacent muscle tissue (SI_{adj}). These measurements were obtained close to the vessel to minimize the error that might occur owing to inhomogeneities of the magnetic field. Absolute SI measurements were related to noise, which was defined as the standard deviation of SI measurements (STD_{noise}) in the background outside of the body (ie, air). SNR and CNR values were calculated from SI and mean STD measurements as follows: $SNR = SI_{ves}/STD_{noise}$, and $CNR = (SI_{ves} - SI_{adj})/STD_{noise}$.

Since we expected to calculate a negative CNR value owing to the lower SI of the nonenhanced venous segment, as compared with the SI of the adjacent tissue, absolute values were considered in the calculations.

Statistical Analyses

A statistics package (SPPS, version 10.0 for Windows; SPSS, Chicago, Ill) was used for subsequent statistical analyses. To assess correlations among the semiquantitative data on overall image quality, degree of stenosis measured in the high-spatial-resolution protocol followed with and without venous compression, and degree of agreement between DSA and MR angiographic results, the Wilcoxon signed rank test was performed. Comparisons of measured SNRs and CNRs between the venous compression and non–venous compression protocols were performed by using the paired-samples *t* test. $P < .05$ was considered to indicate a significant difference. For analysis of the reviewers' rankings of relative image quality, the paired Wilcoxon signed rank test was used.

Results

All subjects tolerated the MR angiographic examination well, without complaints of discomfort or pain due to cuff inflation for venous compression. Quantitative analysis revealed no significant differences between the SNR and CNR values of arterial segments imaged with and those of segments imaged without venous compression ($P > .1$) (Table 2). Mean SNR values were 62.2 (range, 20.0–150.0) with and 61.2 (range, 22.1–139.1) without venous compression; mean CNR values were 51.3 (range, 16.8–128.2) without and 52.4 (range, 14.6–133.3) with venous compression. However, there were significant differences ($P < .05$) in mean SNR values between the venous segments imaged with (7.8; range, 3.8–18.3) and those imaged without (18.5; range, 3.9–55.8) venous compression. The mean CNR values for venous segments were 4.6 (range, 0.2–18.3) with and 9.7 (range 0–55.8) without venous compression (Table 3).

Assessment of image quality revealed significantly higher values for extremities imaged with venous compression, as compared with those for extremities imaged without venous compression (Fig 1): 2.9 ± 0.12 with versus 2.1 ± 0.87 without venous compression ($P < .05$). Differences were even more apparent when the comparison was limited to the most caudal anatomic segments (data sets for the two lowest regions): 2.9 ± 0.14 with versus 1.7 ± 0.82 without venous compression ($P < .05$) (Fig 2).

Of the 220 potentially visible arterial segments in the five examined patients, 43 (19.5%) were not adequately depicted at DSA: two dorsal foot (Fig 3), two medial plantar, two lateral plantar, four deep palmar arch, and 33 metatarsal arterial segments. One hundred seventy-seven arterial segments were well seen at DSA. One hundred thirty-two of these segments were characterized as normal. Abnormalities were identified in 45 segments: 12 segments had vessel irregularities with 50% or less stenosis, eight had more than 50% stenosis, and 25 were occluded.

At MR angiography, 48 (21.8%) of the 220 potentially visible segments were not adequately visualized, largely because of severe venous overlap. In the extremities imaged without venous compression, 42 (38.1%) of the 110 segments were not seen: three distal posterotibial, three distal peroneal, one dorsal foot, six deep palmar arch, four medial plantar, three lateral plantar, and 22 metatarsal arterial segments. In the extremities imaged with venous compression, only six metatarsal arteries (5.4%) were not depicted.

The results for extremities imaged at MR angiography without venous compression are compared with those for extremities imaged at conventional DSA in Table 4. Both DSA and MR angiography depicted severe (>50%) stenosis in three segments and occlusion in nine segments. With MR angiography, four segments were overgraded and two were undergraded.

We observed better correlations between the DSA and MR angiographic results in the extremities imaged at MR angiography with venous compression: Six segments were classified as mildly (≤50%) stenotic; five segments, as severely (>50%) stenotic; and 12 segments, as occluded with both techniques (Table 5). Only two segments were undergraded at MR angiography.

When we combined the results indicating severe stenoses with those indicating occlusion, the overall sensitivities and specificities for the detection of lesions associated with hemodynamically significant arterial disease were 95% (18 of 19 segments) and 100% (63 of 63 segments), respectively, with venous compression and 92% (12 of 13 segments) and 96% (48 of 50 segments), respectively, without venous compression. The calculated Cohen κ values indicating the level of concordance between DSA and

TABLE 2
Mean SNR and CNR Values in Lower Extremity Arterial Vessels Evaluated at High-Spatial-Resolution MR Angiography with and without Venous Compression

	MR Angiography with Venous Compression		MR Angiography without Venous Compression	
Artery*	SNR	CNR	SNR	CNR
Infrarenal aorta	71.1	64.8	71.1	64.8
Common Iliac artery	56.3	50.1	57.2	51.1
External Iliac artery	44.2	39.3	46.1	40.8
Common femoral artery	78.2	71.0	83.9	76.6
Proximal SFA	47.3	41.8	48.3	42.9
Distal SFA	71.2	64.5	75.0	67.7
Popliteal artery	111.6	101.2	97.1	86.9
Tibioperoneal artery	68.0	60.3	64.0	58.1
Proximal anterotibial artery	53.0	45.2	53.4	45.2
Distal anterotibial artery	65.1	55.4	64.3	53.7
Proximal peroneal artery	32.6	28.7	27.4	22.6
Distal peroneal artery	30.6	25.7	27.1	22.5
Proximal posterotibial artery	27.5	23.0	23.9	18.9
Distal posterotibial artery	26.3	20.9	26.8	21.0
Dorsal artery of foot	74.0	56.5	76.7	62.7
Palmar arterial arch	88.5	64.4	89.0	65.2
Plantar metatarsal artery	30.4	24.7	30.0	23.4
Medial plantar artery	81.9	58.5	81.0	54.9
Lateral plantar artery	124.0	98.8	121.3	96.5

* SFA = superficial femoral artery.

TABLE 3
Mean SNR and CNR Values in Lower Extremity Veins Evaluated at High-Spatial-Resolution MR Angiography with and without Venous Compression

	MR Angiography with Venous Compression		MR Angiography without Venous Compression	
Vein	SNR	CNR	SNR	CNR
Common iliac	5.2	0.2	6.6	1.9
Common femoral	5.1	3.3	7.2	1.7
Distal femoral	5.3	1	8.1	0.8
Popliteal	9.8	1.7	17.4	6.6
Proximal peroneal	9.6	4.9	18.6	14.0
Lateral plantar	12.1	16.4	48.6	33.3

Note.—Since negative CNR values due to the lower SI of nonenhanced venous vessel segments, as compared with the SI of adjacent tissue, were expected, absolute values were considered in the calculations of CNR.

a.

b.

Figure 1. Peripheral MR angiograms (for the four stations, repetition times: 2.36, 2.96, 2.96, and 3.77 msec; echo times: 0.96, 0.97, 1.25, and 1.37 msec; flip angle: 20°; field of view: 350–375 × 400 mm; numbers of sections acquired: 48, 88, 64, and 120; section thicknesses: 3.33, 1.56, 1.51, and 1.51 mm interpolated to 2, 1, 1, and 1 mm, respectively; interpolated matrices: 460 × 768, 422 × 768, 952 × 1024, and 757 × 1024; acquisition times: 13, 15, 24, and 44 seconds; parallel imaging factor of 2 used for last three of the four stations) obtained in 32-year-old healthy male volunteer. High-spatial-resolution 3D **(a)** anteroposterior MR angiogram of entire peripheral vascular tree and **(b)** oblique MR angiogram of the inframalleolar vessels, including the pedal arch, obtained with the dedicated peripheral coil are shown. Implementation of midfemoral venous compression in the right leg leads to improved delineation of the arterial morphologic structures, especially the infrapopliteal vessels to the pedal arch.

MR angiographic results were 0.95 for the agreement achieved with and 0.81 for the agreement achieved without venous compression.

Discussion

Current technique refinements permit an all-encompassing diagnostic depiction of the lower extremity arterial system, including the trifurcation and pedal vessels, with MR angiography. Dedicated surface coils ensure sufficient SNRs to support voxel sizes smaller than 0.5 × 0.5 × 1.0 mm^3. Image data sets are based on high-spatial-resolution 3D acquisitions with integrated parallel acquisition algorithms and zero interpolation. Despite lengthy data acquisition times exceeding 100 seconds, arterial phase imaging without venous overlap can be performed by using midfemoral venous compression.

The diagnostic depiction of the lower extremity arteries is based on the fulfillment of the following competing requirements: depiction of the entire arterial system, from the pelvis to the metatarsal arteries, with high spatial resolution and no venous overlap. However, timing issues have precluded the simultaneous fulfillment of these requirements. Although extended imaging coverage and high spatial resolution necessitate lengthy data acquisition times, venous overlap is avoided only when the data acquisition time is limited to the short intraarterial phase. As shown in this study, venous compression provides a solution to this dilemma.

The implementation of bolus chase techniques has led to extended imaging coverage far beyond that of a single body region. Different protocols involving the use of a body coil or dedicated surface coils for data collection have been evaluated. Reported sensitivities and specificities for the detection of stenotic disease range between 85% and 98% for femoral and popliteal vessels. Reflective of vastly decreased arterial diameters, considerably lower sensitivities and specificities for the evaluation of distal infrapopliteal and pedal vessels have been reported (7,8,19,20).

Better spatial resolution requires higher SNRs and CNRs. Greater than 400% increases in these values are possible with the implementation of dedicated peripheral-array coils (11,12). With such high degrees of SI, the voxel sizes of the underlying 3D data sets can be reduced sufficiently, both in the plane and through the plane, to ensure adequate delineation of the small arteries in the calves and feet. Higher spatial resolution, however, requires more data collection and thus results in longer repetition times. Because of the relatively short intraarterial contrast phase, prolonged imaging time results in an overlap of the arterial and venous phases, which has been reported to be present in up to 60% of examinations (19–22). Such overlap, if severe, prevents the isolated identification of the arteries and thereby reduces the diagnostic accuracy.

Different strategies to achieve high spatial resolution at MR angiography of the peripheral arteries without venous overlap have been under investigation. These strategies include approaches to optimize contrast material administration in terms of amount and injection rate, as well as attempts to shorten imaging times (9,20,23–26).

In this study, contrast material was administered by using a biphasic injection protocol. This strategy enables one to quickly achieve maximal arterial enhancement and to maintain this enhancement level for an extended period. Although table motion and 3D data collection do not keep pace with the leading edge of the contrast material bolus, bolus chase MR angiography can be performed

in up to 45 seconds without risk of excessive venous overlap. This capability reflects the long interval between arterial and venous enhancement, which is on the order of 45 seconds (27). However, substantial patient-to-patient variation in contrast material travel times due to conditions such as cellulitis, ulceration, asymmetric occlusion disease, and aneurysm have been reported.

Furthermore, acquisition times for conventional high-spatial-resolution bolus chase MR angiography of the pelvis to the pedal arteries easily exceed 2 minutes (21). Thus, venous overlap remains a limiting factor in the acquisition of entire data sets with high diagnostic accuracy (19).

Several attempts to reduce the imaging time in the setting of high-spatial-resolution contrast-enhanced MR angiography have been made. Shortened repetition times are limited by gradient performance, which in turn is hindered by physical and physiologic constraints (15). With use of parallel acquisition techniques (eg, GRAPPA, sensitivity encoding, and simultaneous acquisition of spatial harmonics), one can at least partly compensate for the ensuing lengthened data acquisition times. Data acquisition speed can be increased by using multiple phased-array coils with known sensitivities (14).

In this study, the GRAPPA technique was used. With this technique, one uses the spatial information contained in individual elements of a phased-array coil before the Fourier transformation to partially replace the phase-encoding steps that normally would be performed by using gradients. Generally, it has been found that the intrinsically high SNR that is achievable at contrast-enhanced imaging enables a twofold acceleration of contrast-enhanced MR angiographic examinations of diagnostic quality (28,29). Accordingly, an acceleration factor of 2 was implemented for the lower three stations in this study. Despite use of the GRAPPA technique, the time required to obtain one high-spatial-resolution 3D image data set in the lower leg region increased from 13 to 44 seconds.

In this study, the time to image the entire peripheral vascular tree still exceeded 100 seconds, despite the use of minimal repetition times with the latest hardware and software, parallel imaging reconstruction, a dedicated peripheral coil with the floating-table technique, partial k-space reconstruction, zero interpolation in the section-select direction, and a biphasic injection protocol. On the

Figure 2. *A,* Nonselective intraarterial DSA image, and, *B,* 3D maximum intensity projection obtained with contrast-enhanced MR angiography (for the four stations, repetition times: 2.36, 2.96, 2.96, and 3.77 msec; echo times: 0.96, 0.97, 1.25, and 1.37 msec; flip angle: 20°; field of view: 350–375 × 400 mm; numbers of sections acquired: 48, 88, 64, and 120; section thicknesses: 3.33, 1.56, 1.51, and 1.51 mm interpolated to 2, 1, 1, and 1 mm, respectively; interpolated matrices: 460 × 768, 422 × 768, 952 × 1024, and 757 × 1024; acquisition times: 13, 15, 24, and 44 seconds; parallel imaging factor of 2 used for last three of the four stations) and dedicated peripheral coil in the lower extremities of 51-year-old female patient with peripheral arterial occlusive disease (Rutherford grade III, category 5). For MR angiography, venous compression was applied to the left leg. Note the better depiction of the left leg infrapopliteal arteries, including the pedal arch, in *B,* as compared with the depiction of these arteries in *A*. However, in the right leg in *B,* venous overlay hampers visualization of the distal vessels.

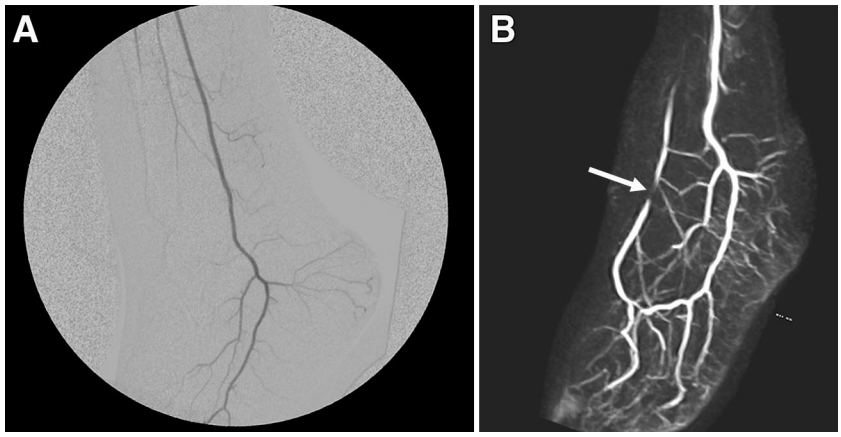

Figure 3. Oblique views of runoff vessels in same patient as in Figure 2. *A,* Intraarterial nonselective DSA image does not show the dorsal artery of the foot. *B,* MR angiogram (3.77/1.77 [repetition time msec/echo time msec], 20° flip angle, 350 × 400 field of view, 120 sections acquired, section thickness of 1.51 mm interpolated to 1.00 mm, matrix of 358 × 512 interpolated by means of zero filling to 757 × 1024, acquisition time of 44 seconds) shows proximal high-grade (>50%) stenosis (arrow) of the dorsal artery of the foot. Note the patent middle and distal segments of the vessel and the runoff vessels to the pedal arch.

TABLE 4
Stenosis Grading at MR Angiography without Venous Compression and at DSA

	MR Angiography				
DSA	No Stenosis	≤50% Stenosis	>50% Stenosis	Occlusion	Total
No stenosis	48	2	0	0	50
≤50% stenosis	1	2	2	0	5
>50% stenosis	0	0	3	0	3
Occlusion	0	1	0	9	10
Total	49	5	5	9	68

Note.—Data are numbers of vessel segments. Two observers in consensus determined the stenosis grades of the vessel segments.

TABLE 5
Stenosis Grading at MR Angiography with Venous Compression and at DSA

	MR Angiography				
DSA	No Stenosis	≤50% Stenosis	>50% Stenosis	Occlusion	Total
No stenosis	63	0	0	0	63
≤50% stenosis	0	6	0	0	6
>50% stenosis	0	0	5	0	5
Occlusion	0	1	1	12	14
Total	63	7	6	12	88

Note.—Data are numbers of vessel segments. Two observers in consensus determined the stenosis grades of the vessel segments.

basis of such long time requirements, venous overlap seems unavoidable. A frequently proposed solution involves the separate, often time-resolved, acquisition of images of the calf and pedal vessels (30). Although this technique has been shown to provide excellent results, it has had a limited clinical effect owing to complex and time-consuming protocol adjustments and lengthy data reconstruction times. Furthermore, an additional contrast material dose is required.

The proposed venous compression technique enables one to overcome the limitations inherent to separate and time-resolved examinations while avoiding venous overlap. Complete high-spatial-resolution imaging coverage of the lower extremity arterial system can be achieved in a single examination with one administration of contrast material. Venous compression at imaging of the lower extremity arteries represents a modification of a technique recently proposed by Wentz et al (31) for high-spatial-resolution MR angiography of the upper extremities. Inflating a cuff to 200 mm Hg after the arterial inflow of contrast material caused blood flow to be completely interrupted and thus left sufficient time for high-spatial-resolution imaging of the arm.

Because cuff inflation up to 200 mm Hg is not tolerated well by patients with peripheral arterial occlusive disease of the lower extremities, we reduced the cuff inflation to 50 mm Hg. This level of pressure blocked the venous blood flow without impairing arterial blood flow to the pedal arch. This technique does not cause ischemic pain and is easier to implement than is the technique described by Wentz et al (31) because cuff insufflation can be performed before contrast material administration without paying attention to the inflow of the compound into the investigated vascular territory. As shown by the present study results, the effect in terms of eliminating venous overlap was not compromised. The effect of compression to the leg on the contrast material travel time cannot be attributed to venous compression alone; rather, we believe the effect is related to an intermediate reactive hyperemia that is created in peripheral tissue by the compression. Thus, the extracellular space is increased, leading to a prolonged interval between arterial and venous enhancement.

The present study had several limitations. First and most important, the lack of selective catheterization compromised the standard-of-reference results. Thus, the documented superiority of contrast-enhanced high-spatial-resolution MR angiography with venous compression relative to DSA in the identification of patent arterial segments of the infrapopliteal and runoff vessels of the feet needs to be interpreted with care. Furthermore, the numbers of examined volunteers and patients were very limited. This factor was offset at least to some degree by our ability to perform intraindividual comparisons. When venous compression is used in a large number of patients, it may induce venous thrombosis in a few of them; however, the risk is small. Therefore, the applicability of the described venous compression technique in pa-

tients with severe peripheral vascular disease needs to be studied in a larger cohort.

It may, in certain cases, be impossible to eliminate venous contamination. Small arteriovenous fistulas are not uncommonly seen at conventional selective DSA. Therefore, one can expect to be hampered by these passages at contrast-enhanced MR angiography as well. Still, our study results need to be validated in larger patient cohorts. However, on the basis of the data presented herein, we conclude that high-spatial-resolution MR angiography of the peripheral arterial system, including the pedal arteries, is possible with use of a refined data acquisition technique that includes the application of midfemoral venous compression to minimize venous overlap.

References

1. Rofsky NM, Johnson G, Adelman MA, Rosen RJ, Krinsky GA, Weinreb JC. Peripheral vascular disease evaluated with reduced-dose gadolinium-enhanced MR angiography. Radiology 1997; 205:163–169.
2. Prince MR, Narasimham DL, Stanley JC, et al. Breath-hold gadolinium-enhanced MR angiography of the abdominal aorta and its major branches. Radiology 1995; 197:785–792.
3. Snidow JJ, Aisen AM, Harris VJ, et al. Iliac artery MR angiography: comparison of three-dimensional gadolinium-enhanced and two-dimensional time-of-flight techniques. Radiology 1995; 196:371–378.
4. Ruehm SG, Hany TF, Pfammatter T, Schneider E, Ladd M, Debatin JF. Pelvic and lower extremity arterial imaging: diagnostic performance of three-dimensional contrast-enhanced MR angiography. AJR Am J Roentgenol 2000; 174:1127–1135.
5. Hany TF, Debatin JF, Leung DA, Pfammatter T. Evaluation of the aortoiliac and renal arteries: comparison of breath-hold, contrast-enhanced, three-dimensional MR angiography with conventional catheter angiography. Radiology 1997; 204: 357–362.
6. Earls JP, DeSena S, Bluemke DA. Gadolinium-enhanced three-dimensional MR angiography of the entire aorta and iliac arteries with dynamic manual table translation. Radiology 1998; 209:844–849.
7. Ho KY, Leiner T, de Haan MW, Kessels AG, Kitslaar PJ, van Engelshoven JM. Peripheral vascular tree stenoses: evaluation with moving-bed infusion-tracking MR angiography. Radiology 1998; 206:683–692.
8. Meaney JF, Ridgway JP, Chakraverty S, et al. Stepping-table gadolinium-enhanced digital subtraction MR angiography of the aorta and lower extremity arteries: preliminary experience. Radiology 1999; 211:59–67.
9. Swan JS, Carroll TJ, Kennell TW, et al. Time-resolved three-dimensional contrast-enhanced MR angiography of the peripheral vessels. Radiology 2002; 225: 43–52.
10. Wang Y, Lee HM, Khilnani NM, et al. Bolus-chase MR digital subtraction angiography in the lower extremity. Radiology 1998; 207:263–269.
11. Janka R, Fellner F, Fellner C, et al. Dedicated phased-array coil for peripheral MRA. Eur Radiol 2000; 10:1745–1749.
12. Goyen M, Ruehm SG, Barkhausen J, et al. Improved multi-station peripheral MR angiography with a dedicated vascular coil. J Magn Reson Imaging 2001; 13:475–480.
13. Alson MD, Lang EV, Kaufman JA. Pedal arterial imaging. J Vasc Interv Radiol 1997; 8:9–18.
14. Sodickson DK, McKenzie CA, Li W, Wolff S, Manning WJ, Edelman RR. Contrast-enhanced 3D MR angiography with simultaneous acquisition of spatial harmonics: a pilot study. Radiology 2000; 217:284–289.
15. Weiger M, Pruessmann KP, Kassner A, et al. Contrast-enhanced 3D MRA using SENSE. J Magn Reson Imaging 2000; 12: 671–677.
16. Bilecen D, Aschwanden M, Heidecker HG, Bongartz G. Optimized assessment of hand vascularization on contrast-enhanced MR angiography with a subsystolic continuous compression technique. AJR Am J Roentgenol 2004; 182: 180–182.
17. Dormandy JA, Rutherford RB. Management of peripheral arterial disease (PAD). TASC Working Group. TransAtlantic Inter-Society Concensus (TASC). J Vasc Surg 2000; 31:S1–S296.
18. Griswold MA, Jakob PM, Heidemann RM, et al. Generalized autocalibrating partially parallel acquisitions (GRAPPA). Magn Reson Med 2002; 47:1202–1210.
19. Foo TK, Ho VB, Hood MN, Marcos HB, Hess SL, Choyke PL. High-spatial-resolution multistation MR imaging of lower-extremity peripheral vasculature with segmented volume acquisition: feasibility study. Radiology 2001; 219:835–841.
20. Hany TF, Carroll TJ, Omary RA, et al. Aorta and runoff vessels: single-injection MR angiography with automated table movement compared with multiinjection time-resolved MR angiography—initial results. Radiology 2001; 221:266–272.
21. Wang Y, Chen CZ, Chabra SG, et al. Bolus arterial-venous transit in the lower extremity and venous contamination in bolus chase three-dimensional magnetic resonance angiography. Invest Radiol 2002; 37:458–463.
22. Wang Y, Winchester PA, Khilnani NM, et al. Contrast-enhanced peripheral MR angiography from the abdominal aorta to the pedal arteries: combined dynamic two-dimensional and bolus-chase three-dimensional acquisitions. Invest Radiol 2001; 36:170–177.
23. Carroll TJ, Korosec FR, Swan JS, Hany TF, Grist TM, Mistretta CA. The effect of injection rate on time-resolved contrast-enhanced peripheral MRA. J Magn Reson Imaging 2001; 14:401–410.
24. Kita M, Mitani Y, Tanihata H, et al. Moving-table reduced-dose gadolinium-enhanced three-dimensional magnetic resonance angiography: velocity-dependent method with three-phase gadolinium infusion. J Magn Reson Imaging 2001; 14:319–328.
25. Czum JM, Ho VB, Hood MN, Foo TK, Choyke PL. Bolus-chase peripheral 3D MRA using a dual-rate contrast media injection. J Magn Reson Imaging 2000; 12: 769–775.
26. Wyttenbach R, Gianella S, Alerci M, Braghetti A, Cozzi L, Gallino A. Prospective blinded evaluation of Gd-DOTA– versus Gd-BOPTA–enhanced peripheral MR angiography, as compared with digital subtraction angiography. Radiology 2003; 227:261–269.
27. Prince MR, Chabra SG, Watts R, et al. Contrast material travel times in patients undergoing peripheral MR angiography. Radiology 2002; 224:55–61.
28. Maki JH, Wilson GJ, Eubank WB, Hoogeveen RM. Utilizing SENSE to achieve lower station sub-millimeter isotropic resolution and minimal venous enhancement in peripheral MR angiography. J Magn Reson Imaging 2002; 15:484–491.
29. Sodickson DK, Griswold MA, Jakob PM, Edelman RR, Manning WJ. Signal-to-noise ratio and signal-to-noise efficiency in SMASH imaging. Magn Reson Med 1999; 41:1009–1022.
30. Kreitner KF, Kalden P, Neufang A, et al. Diabetes and peripheral arterial occlusive disease: prospective comparison of contrast-enhanced three-dimensional MR angiography with conventional digital subtraction angiography. AJR Am J Roentgenol 2000; 174:171–179.
31. Wentz KU, Frohlich JM, von Weymarn C, Patak MA, Jenelten R, Zollikofer CL. High-resolution magnetic resonance angiography of hands with timed arterial compression (tac-MRA). Lancet 2003; 361:49–50.